Power Electronics for an Energy Harvesting Concept Applied to Magnetic Resonance Tomography

L. Middelstaedt[1], S. Foerster[2], R. Doebbelin[1], and A. Lindemann[1]

[1]Otto-von-Guericke-University Magdeburg, Germany
[2]formerly Otto-von-Guericke-University Magdeburg, Germany

Abstract— In this paper the possibility of utilizing magnetic fields of magnetic resonant imaging (MRI) scanners for energy harvesting is investigated. The magnetic energy is converted into electric energy supplying small sensor systems that can be used for interventional medical applications within an MRI scanner. Suitable magnetic field components for energy harvesting are analyzed and a corresponding inductor design is discussed. Accordingly, a power electronic circuit is developed and successfully tested within an MRI scanner wirelessly powered by an inductor.

1. INTRODUCTION

Concerning the power supply of small power electronic applications for devices used in the interventional medical field in magnetic resonance tomography (MRT), e.g., for wireless power supply of small sensors and electronics in catheters, this paper investigates the approach of energy harvesting inside the MRI scanner. While in [1] basic investigations on energy harvesting in MRT were carried out by measuring the DC output power for one setup, this paper investigates and evaluates the induction coil design in more detail by determining the induced voltage and the self resonances of the inductors. Additionally, the time variant magnetic RF field and the gradient field are compared in terms of induced voltage depending on the induction coil placement relative to the isocenter, which is the geometrical center of the magnet where the static magnetic field and the RF field are the strongest and homogenous.

2. ANALYSIS OF MAGNETIC FIELDS IN MRT

In order to supply an electronic circuit using energy harvesting within an MRI scanner, suitable magnetic fields need to be defined and analyzed.

2.1. Magnetic Fields in MRT

Within magnetic resonance tomography (MRT) applications magnetic fields of different orientations, magnitudes and frequencies are generated in order to produce images of different body tissues. The three main magnetic fields that need to be distinguished are [2–4]:

- B_0: strong static, uniform magnetic field in z direction.
- B_1: high frequency excitation field ($\approx 123\,\mathrm{MHz}$ for $B_0 = 2.89\,\mathrm{T}$ according to Larmor frequency [5]) rotating in the xy plane and having the highest amplitude in the isocenter.
- B_G: gradient field with x, y, and z components with location-depending characteristics.

Figure 1 shows the corresponding geometry definitions. Considering the magnetic fields and according to Faraday's Law, the B_1 and B_G fields can be utilized to convert portions of the magnetic energy into electric energy, as stated in [1] as well.

2.2. Field Simulation

To investigate the induction behavior of inductor with different geometries excited by the B_1 field, a numerical field simulation model was created in EMPIRE XCcel$^{\mathrm{TM}}$. B_1 is homogenous and rotates in the xy plane with a frequency of approximately 123 MHz. To create a magnetic field with these characteristics in EMPIRE XCcel$^{\mathrm{TM}}$ four electromagnetic (EM) waves are superimposed, so that the electric field components cancel out and the resulting homogenous H field is rotating in the xy plane. Therefore, the amplitudes of the electric components $\vec{E}$ of the four EM waves have to be equal. Two contrary polarized EM waves having opposite direction of propagation $\vec{k}$ with

$$\vec{k} = \vec{E} \times \vec{H} \tag{1}$$

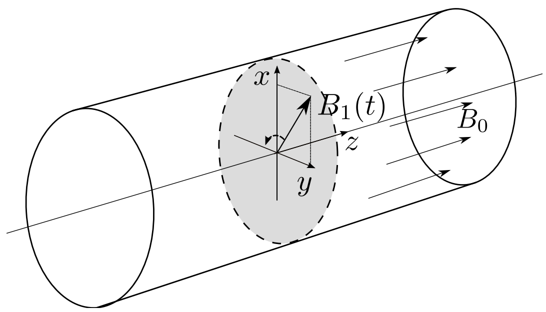

Figure 1: Definition of axes within an MRI scanner and corresponding magnetic fields.

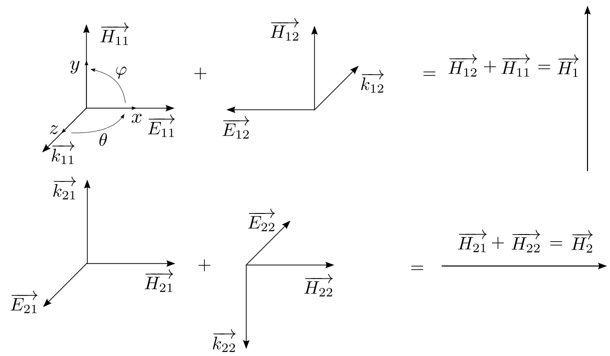

Figure 2: Orientation of two pairs of electromagnetic waves, resulting in two homogenous H fields.

are added and result in one homogenous H field with an orientation as shown in Figure 2. Adding the two homogenous H fields $\overrightarrow{H_1}$ and $\overrightarrow{H_2}$ rotated relatively to each other geometrically and electrically by 90° results in a single circularly polarized homogenous H field. To realize a 90° phase shift between $\overrightarrow{H_1}$ and $\overrightarrow{H_2}$ for ≈ 123 MHz a time delay of 2.0316 ns needs to be applied.

With the model of B_1 the induction characteristic of different geometries can be analyzed and compared. It is important, that the defined simulation geometry is smaller than the wave length of the B_1 field. For larger geometries the superposition of the four EM waves does not result in one circularly polarized homogenious H field.

3. LAYOUT AND DESIGN OF PROTOTYPE

3.1. Inductor Design

For the inductor design different considerations need to be taken into account, i.e., the orientation, frequency and strength of the exciting magnetic field. As already mentioned, the frequency of the B_1 field equals ≈ 123 MHz and it rotates in the xy plane at the location of the isocenter. Here, the field strength is the highest and depends on the sequence of the MRT that is applied. However, the absolute amplitude of B_1 is small and hence a large number of turns might by plausible. Contrary, a large number of turns increases the effect of capacitive coupling between turns and therefore decreases the first resonant frequency of the inductor [6]. Only below the first resonant frequency, the inductor behaves strongly inductive. For higher frequencies the parasitic capacitive component may become dominant and hence the induced output voltage decreases. An optimization is reached, when the first resonant frequency is slightly above the excitation frequency.

Additionally, the inductor can be optimized by maximizing the effective area, that is exposed to the magnetic field. Since the direction of excitation varies between the x and y axes it is desired to design the winding in a way, that the inductor is excited by the B_1 field from both components considering that the area which is orthogonal to the varying field represents the effective area of the inductor. While in literature inductors with different coils for each orientation [4] or a Figure 8 coil with one orientation [7] are described, this paper proposes an approach that uses only one coil with tilted turns wound around an acrylic glass tube. The turns are arranged with a 45° angle (see Figure 3).

In Figure 4 different orientations are displayed. For orientation 1 and orientation 2 the inductor

Figure 3: Prototype induction coil with 100 turns on cylindrical acrylic tube.

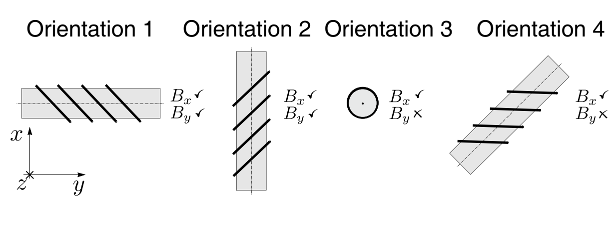

Figure 4: Orientation of winding setup on an acrylic glass tube concerning exciting B field components.

is excited by the x and y component of the exciting B_1 field. For the other orientations only the excitation by B_x is given. However, for orientation 3 the x-excitation is possible only because of the tilted turns. For orientation 4 the tilted turns lead to an elliptic area, which is larger than a circular area. Thus, the increased effective area leads to an increased inductance and therefore increased induced voltage.

3.2. Power Electronic Circuit Design

The inductor is used as a wireless AC voltage source. In order to supply small power electronic applications like sensors a low DC voltage is needed. Hence, the input voltage needs to be converted using a power electronic circuit. In the first stage the input voltage is rectified with diodes and buffered using a capacitor. Due to the fluctuation of buffered voltage a DC-DC converter with charging management is used in the second stage, to achieve a constant output voltage. The block diagram of the circuit is shown in Figure 5. The circuit charges an output buffer capacitor and supplies an LED with an ohmic resistance in series.

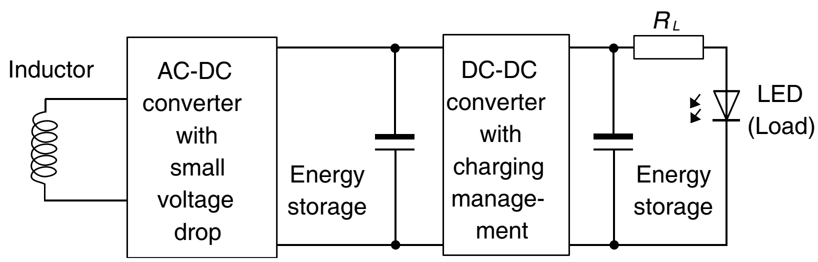

Figure 5: Block diagram of the power electronic circuit supplying an LED [8].

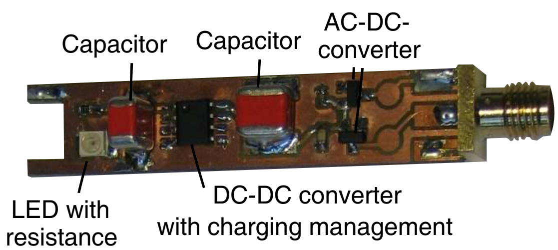

Figure 6: Assembeled circuit board with electronic elements.

Figure 7: Prototype with inductor and circuit board.

For the use in MRT applications, e.g., for interventional medical use, the circuit needs to fulfill different requirements. Next to a small size, the voltage drop over the circuit elements needs to be as small as possible to ensure a high efficiency. Furthermore, the imaging process of the MRT should not be affected, requiring the circuit elements to be of non-magnetic material. Widely used electronic elements with nickel alloys for solder connections can not be applied. Elements with a copper-tin-zinc alloy serve as a substitute. Different supliers, e.g., Maxim or Texas Instruments, have developed highly integrated circuits for energy harvesting applications, that offer a DC-DC converter with additional charging management and different protection and charging controls combined in a minimized package of only approximately 9 mm^2. The prototype uses such an IC that is soldered onto a circuit board (see Figure 6). The board was slid into the inductor in order to reduce size and create a compact device as displayed in Figure 7. An SMA socket is used to connect a measurement cable with the device to measure the induced voltage.

4. RESULTS

The induction characteristics of two inductors with different numbers of turns were compared. For inductor 1 100 turns were applied, whereas inductor 2 has only six turns. The impedance characteristic at the exciting frequency of $\approx$ 123 MHz is of higher importance. At 500 kHz the inductance of inductor 1 is approximately 400 times larger than of inductor 2. Contrary, at $\approx$ 123 MHz both inductors show an impedance value in the same order of magnitude, as can be seen from Table 1. The phase angles show, that the parasitic capacitances of inductor 1 have a major

Table 1: Impedance characteristic of inductors at $\approx 123\,\mathrm{MHz}$.

	Z	φ
Inductor 1	$200\,\Omega$	$-70°$
Inductor 2	$450\,\Omega$	$87°$

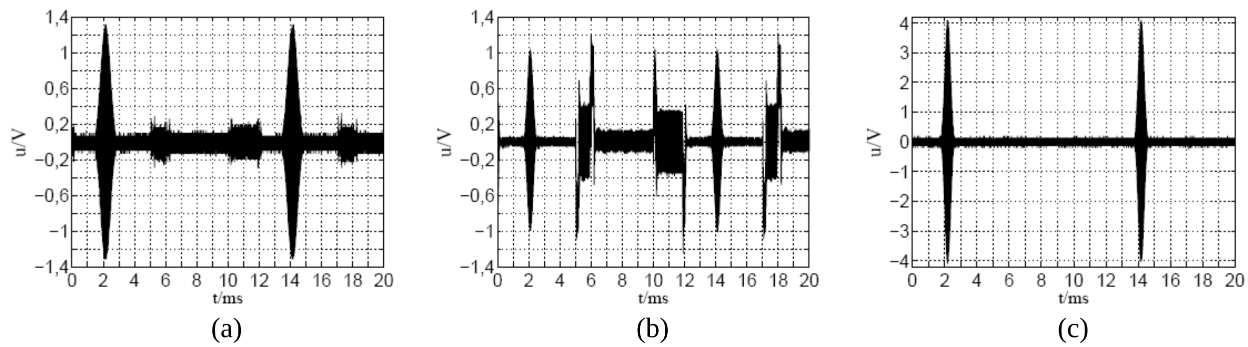

Figure 8: Induced voltage for different inductors at different positions. (a) Inductor 1 at isocenter, (b) inductor 1 outside of isocenter, (c) inductor 2 at isocenter.

influence and the impedance characteristic is not inductive any more. On the other hand, inductor 2 still shows a mostly inductive behavior.

Accordingly, the induced voltages differ. In Figure 8 the oscillograms of the induced voltages for both inductors are shown, while the voltage of inductor 1 was measured at different positions in relation to the isocenter. The periodicity of the three measurements is the same. At 2 ms and 14 ms the B_1 field induces a voltage. At 5 ms, 10 ms, and 18 ms the gradient field B_G shows its influence. Inductor 1 was placed at the isocenter as well as approximately 20 cm outside of it. Since B_1 is the strongest here, the corresponding induced voltage is the highest with 1.4 V and oscillates with $\approx 123\,\mathrm{MHz}$. The voltages induced by B_G are negligible. Placing the inductor 1 outside of the isocenter leads to a reduction of the induced voltage related to B_1 but increases the induced voltages related to B_G considerably (see Figure 8(b)). In Figure 8(c) inductor 2 was placed at the isocenter and B_1 induces large voltages of 4 V. In this case the reduced number of turns and thus an increased first resonant frequency leads to clearly improved induction characteristic.

This proves, that voltages with sufficient amplitudes are induced at the isocenter as well as outside of it. Not only B_1 but also B_G contribute to the harvesting concept, depending on the position.

Finally, inductor 2 was connected to the power electronic circuit and placed inside the MRI scanner. The magnetic fields lead to an induced voltage that powered the LED wirelessly, which therefore luminates.

5. CONCLUSION

An energy harvesting concept was presented for supplying small low power electronic devices wirelessly for medical applications in an MRI scanner using its magnetic fields. A fundamental simulation was parametrized to model the B_1 field, so that the inductance characteristic of different inductor designs can be simulated and compared.

Then different aspects if the inductor designs were discussed. For an optimized layout a small number of turns is important so that the first resonant frequency of the inductor is higher than the characteristic frequency of the B_1 field. Furthermore, the orientation of the turns is important. An elliptic design was presented, allowing a good induction characteristic independent from the inductors orientation in the magnetic field.

A power electronic circuit was developed, that is able to supply a load consisting of an output buffer capacitance and an LED with resistance. Finally, the prototype was successfully tested within an MRI scanner.

ACKNOWLEDGMENT

The authors would like to thank the State of Sachsen-Anhalt and the German Federal Ministry for Education and Research (BMBF) for supporting our work within the framework of the project Forschungscampus STIMULATE.

REFERENCES

1. Hoefflin, J., E. Fischer, J. Hennig, and J. G. Korvink, "Energy harvesting towards autonomous MRI detection," *Proc. Intl. Soc. Mag. Reson. Med.*, Vol. 21, 2013.
2. Bernstein, M., K. King, and X. Zhou, *Handbook of MRI Pulse Sequences*, Elsevier, 2004.
3. Kuperman, V., *Magnetic Resonance Imaging: Physical Principles and Applications*, Academic Press, 2000.
4. Sun, T., X. Xie, and Z. Wang, *Wireless Power Transfer for Medical Microsystems*, Springer Science+Business Media, New York, 2013.
5. Reiser, M., W. Semmler, and H. Hricak, *Magnetic Resonance Tomography*, Springer-Verlag, Berlin, Heidelberg, 2008.
6. Middelstadt, L., S. Skibin, R. Dobbelin, and A. Lindemann, "Analytical determination of the first resonant frequency of differential mode chokes by detailed analysis of parasitic capacitances," *2014 16th European Conference on Power Electronics and Applications (EPE'14-ECCE Europe)*, 1–10, Aug. 2014.
7. Hoefflin, J., E. Fischer, J. Hennig, and J. G. Korvink, "Energy harvesting with a Figure 8 coil towards energy autonomous MRI detection," *54th Experimental Nuclear Magnetic Resonance Conference*, Apr. 2013.
8. Middelstaedt, L., S. Foerster, and A. Lindemann, "Energy harvesting im MRT," *IGIC, Conference on Image-guided Interventions, Magdeburg*, 2014.